EFFECT OF MICROBUNCHING ON SEEDING SCHEMES FOR LCLS-II

G. Penn, J. Qiang, LBNL, Berkeley, CA 94720, USA

P. Emma, E. Hemsing, Z. Huang, G. Marcus,

T.O. Raubenheimer, L. Wang, SLAC, Menlo Park, CA 94025, USA

Abstract

External seeding and self-seeding schemes are particularly sensitive to distortions and fluctuations in the electron beam profile. Wakefields and the microbunching instability are important sources of such imperfections. Even at modest levels, their influence can degrade the spectrum and decrease the output brightness. These effects are evaluated for seeded FELs at the soft X-ray beam line of LCLS-II. FEL simulations are performed in GENESIS based on various realistic electron distributions obtained using the IMPACT tracking code. The sensitivity depends on both the seeding scheme and the output wavelength.

INTRODUCTION

At LCLS-II [1], the bandwidth is expected to be improved over SASE [2] through the use of self-seeding [3,4] schemes which filter out all but a narrow spectral bandwidth of the radiation somewhere in the middle of the undulators used for FEL amplification. Seeding using external lasers is another means by which a narrow spectrum can be produced, and includes other benefits such as more control over the x-ray pulse. Here we consider the self-seeding and echo-enabled harmonic generation (EEHG) schemes. Self-seeding is already being used at LCLS [5], while EEHG has been demonstrated at NLCTA [6] up to the 15th harmonic (160 nm).

Any attempt to generate coherent x-ray radiation from an electron beam is subject to phase variations caused by longitudinal variations in the electron bunch, through physical effects such as wake fields and the microbunching instability [7]. Laser heaters (LH) are currently used in LCLS to control the microbunching instability, and will be used in LCLS-II as well. In this paper, we consider two settings of the laser heater power, which produce microbunching at substantially different amplitude. The laser heater is set to that a slice energy spread of either 6 keV or 12 keV is produced at the end of the laser heater section, before bunch compression. We then characterize the sensitivity of each FEL scheme to microbunching by comparing the spectrum under these two settings.

The impact of wake fields is considered as well in these studies. When external lasers are used, they are modelled in an idealized fashion because the effect of laser errors is fairly well understood and broadly similar for different seeding schemes, except that EEHG has tighter tolerances on the laser power. It may be possible for carefully optimized lasers to improve performance even further, but because microbunching varies on a shot-by-shot basis there are limited possibilities to counteract this particular effect.

ELECTRON BEAM AND UNDULATOR PARAMETERS

The simulations shown below use particles obtained from start-to-end (S2E) simulations of the injector and linac accelerating the beam to 4 GeV, using the code IMPACT [8]. Previous studies [1,9] used beams derived from ASTRA [10] and ELEGANT [11] which included wake fields and coherent synchrotron radiation (CSR) but only included space charge forces at very low energies. The IMPACT simulations which generated the beams used here track a very large number of particles for higher fidelity, have a full 3D space charge model, and a better algorithm for CSR [12]. The nominal parameters for the electron beam and the main undulator sections for producing radiation are given in Table 1. The longitudinal phase space of the beams are shown in Fig. 1. Note the substantial decrease in levels of microbunching at the higher laser heater settings.

The final undulators have a period of 39 mm and cover a tuning range from 250 eV to 1.3 keV. We study x-ray radiation pulses at 540 eV and 1.2 keV. When external lasers are used, they operate at a wavelength of approximately 260 nm.

Table 1: Example Beam and Undulator Parameters for Soft X-ray Production at LCLS-II

Parameter	Symbol	Value
Electron Beam:		
Bunch charge	Q	300 pC
Electron energy	E	4 GeV
Peak current	I	1 kA
Emittance	ϵ_N	0.43 μm
Energy spread	σ_E	0.5 MeV
Beta function	β	15 m
Final undulators:		
Undulator period	λ_u	39 mm
Undulator segment length	L_{seg}	3.4 m
Break length	L_b	1.2 m
Min. magnetic gap	g_{min}	7.2 mm
Max. undulator parameter	K_{max}	5.48

LAYOUTS FOR DIFFERENT FEL SCHEMES

The layouts for the two main schemes are shown in Fig. 2. FEL simulations were performed using GENESIS [13]. These and other schemes have previously been considered in the LCLS-II Conceptual Design Report [14] for idealized
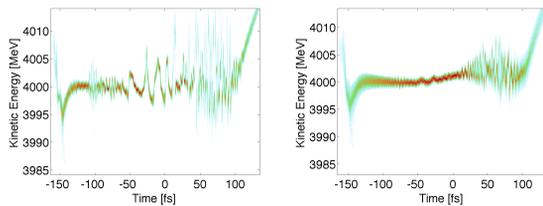
Figure 1: Longitudinal phase space for a 300 pC bunch with the laser heater inducing a 6 kev energy spread (left) and a 12 kev energy spread (right).

beams. Both beamlines should be capable of operating up to photon energies of 1.3 keV. For the self-seeding beamline it may be necessary to detune the first few undulator sections at lower photon energies, because the FEL gain rate is faster and it is undesirable to reach saturation upstream of the monochromator.
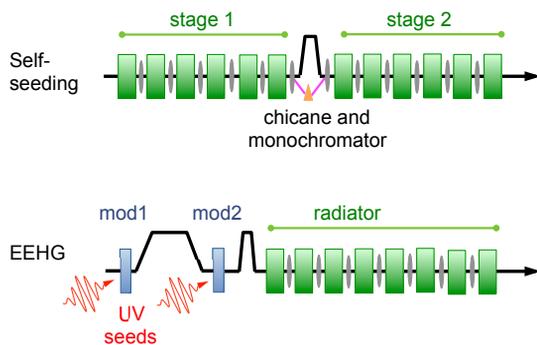

Figure 2: Beamline layouts using self-seeding (top) and EEHG (bottom).

Self-seeding Design and Layout

The self-seeding section is already part of the LCLS-II baseline, and involves only a small modification to the SASE beamline. One of the locations which would otherwise hold an undulator section will instead have a chicane and a monochromator. The chicane will fully debunch the electron beam (any value of $R_{56} \geq 10\,\mu m$ should suffice), and the monochromator will extract the SASE radiation field and allow only a narrow window in the spectrum to return to interact with the beam. The actual strength of the chicane will be adjusted so that the transit time of the electron beam will match that of the radiation field through the monochromator.

Here, we consider a monochromator resolving power of $R = 15000$, defined so that the bandwidth of the filtered radiation pulse will have a fwhm corresponding to $1/R$ of the target photon energy. The actual specifications and final design of the LCLS-II monochromator are still under development. Our current choice of a relatively large value for R is predominantly driven by a desire to highlight any effects which may cause even a small degradation in the bandwidth. We assume an efficiency of 2%; this means that in addition to eliminating out-of-bandwidth radiation, only 2% of the

pulse energy originally within the bandwidth window makes it through the monochromator section due to losses. The monochromator used in LCLS as described in Ref. [5] has a resolving power in the range 2000 to 5000, and an efficiency between 7% and 15%.

EEHG Design and Layout

Echo-enabled harmonic generation (EEHG) [15] mixes modulations from two seed lasers, instead of using only one external laser as in HGHG. The first modulation is followed by a chicane which strongly overbunches the modulation. The chicane after the second modulation typically maximizes the bunching at the wavelength of the input laser. The overall bunching factor can be significant even at very high harmonics using fairly reasonable amplitudes of energy modulation.

Although the external lasers are not required to have the same wavelength, here both seed lasers have identical wavelengths close to 260 nm. The first undulator section is 3.2 m long, with a period of 0.1 m. The second undulator section is also 3.2 m long but with a period of 0.4 m, in order to reduce the amount of energy diffusion due to incoherent synchrotron radiation (ISR). Due to the combination of having fewer periods and sometimes requiring more energy modulation, the second laser needs a much higher peak power, up to 1 GW. To highlight the impact on the bandwidth, we take relatively long laser pulses with 400 fs fwhm. The output pulse is typically 75 fs fwhm.

Similarly, the first chicane has a much larger R_{56} of up to 15 mm, is longer and uses weaker magnets to reduce ISR. There is a tradeoff between reducing ISR and increasing the impact of intrabeam scattering (IBS) by adding to the chicane length.

After the bunching is generated, the electron beam goes directly into undulator sections with a 39 mm undulator period. Radiation is produced at the desired harmonic and amplified to saturation.

SIMULATION RESULTS

We show results for producing radiation at 1.2 keV, near the upper end of the tuning range for soft x-rays at LCLS-II, and at 540 eV. Wakefields are included in the simulation, with a nominal beam pipe diameter of 5 mm. However, because the initial stage of EEHG is especially sensitive to wake fields, and there is a relaxed undulator gap requirement for the modulating undulators, it was found advantageous to increase the beam pipe diameter in that section to 10 mm. Models for IBS were added within the same region, while ISR effects are already included in GENESIS.

The output spectrum profiles for a self-seeding beamline are shown in Fig. 3. The output pulse energy is 125 μJ at 1.2 keV with a 150 fs fwhm duration, and 331 μJ at 540 eV with a 110 fs fwhm duration. It is notable that the radiation at 540 eV is much more severely degraded when there is more microbunching than the radiation at 1.2 keV. For the chosen resolving power of $R = 15000$, the monochromator
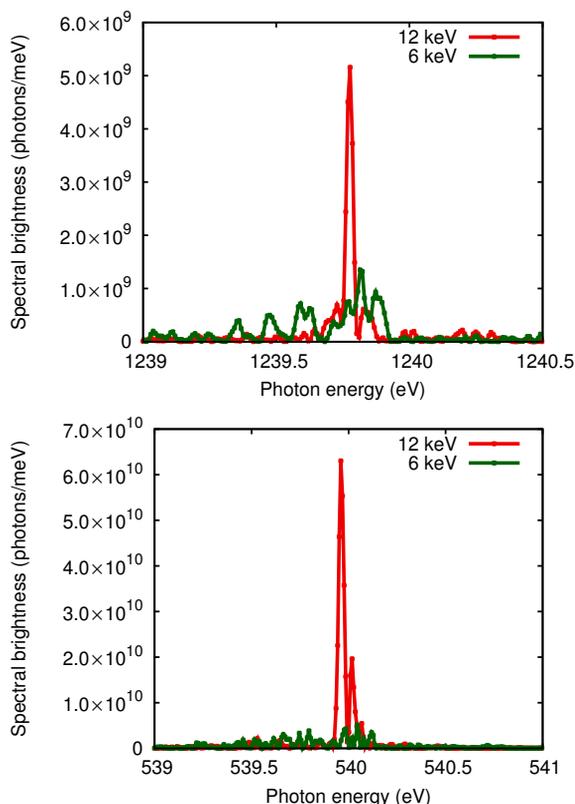
Figure 3: Spectral profiles of the final x-ray pulses for self-seeding, at different wavelengths and for different laser heater (LH) settings.
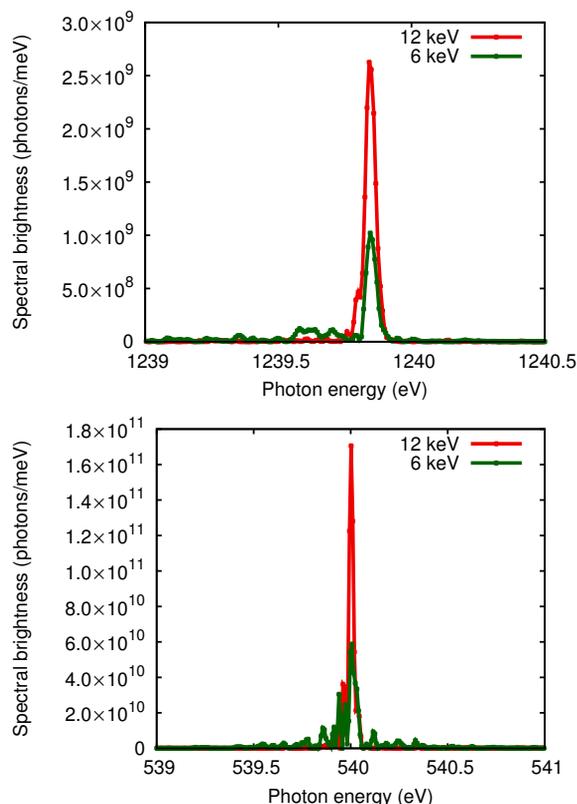
Figure 4: Spectral profiles of the final x-ray pulses for EEHG, at different wavelengths and for different laser heater (LH) settings.

does yield a longer coherence length at the lower photon energy. However, simulations with $R = 7000$ show a similar degradation at 540 eV when comparing the two laser heater settings. There appears to be a fundamental effect which is more of a concern at longer wavelengths than shorter wavelengths.

For EEHG starting from a pair of external lasers at 260 nm, the final x-ray properties are shown in Fig. 4. The output pulse energy is 32 μJ at 1.2 keV with a fwhm duration of 75 fs, and 638 μJ at 540 eV with a fwhm duration of 140 fs. The fwhm bandwidth is less than a factor of 2 from the transform limit when the high laser heater setting is used.

The above spectra are summarized in Fig. 5, in terms of the functional dependence of the fraction of pulse energy contained within a given bandwidth window, as that window is varied. It is particularly notable that for self-seeding, the spectrum at 540 eV with the high laser heater (LH) setting better than both spectra at 1.2 keV, while the spectrum at 540 eV with the low LH setting is worse than both of these spectra. For EEHG, on the other hand, the cumulative fractional energy curves fall into groups depending primarily on the strength of the LH.

CONCLUSION

As expected, seeding schemes perform better at lower harmonic jumps. However, self-seeding simulations show increased sensitivity to microbunching when radiating at longer wavelengths. While there is no harmonic jump in self-seeding, it is still somewhat surprising to see tighter tolerances being required at longer wavelengths. One possible explanation is that the resonance condition requires increased dispersion in the undulators at longer wavelengths. Energy modulations introduce phase modulations during the amplification process, and at low levels phase shifts are proportional to the dispersion and inversely proportional to the wavelength. Thus, the increased dispersion in the undulators should at least balance out the longer wavelength.

Another difference at longer wavelengths is that the FEL parameter is larger, which decreases the importance of the beam energy spreads on the growth rate. It is thus easier for regions of high current and high energy spread to produce significant amounts of unseeded radiation. Microbunching increases the number and amplitude of high current spikes in the beam, and only at shorter wavelengths will damping from the energy spread compensate for the excitation coming from the higher peak current.

The EEHG seeding scheme should produce long pulses with good coherence, assuming that the second seed laser can be tightly controlled. The parameter settings, especially the chicane strengths, must be very carefully set but are fairly robust to variations in electron bunch properties.
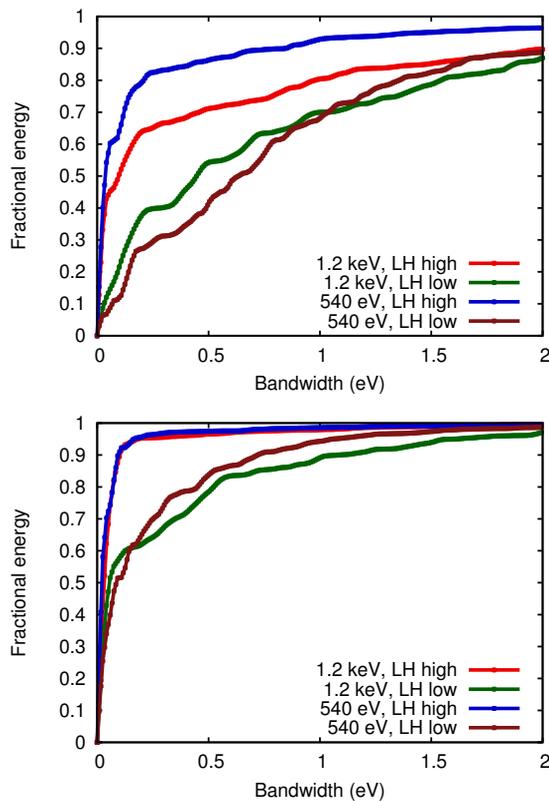
Figure 5: Spectral properties for self-seeding (top) and EEHG (bottom) for various wavelengths and laser heater settings, summarized in terms of the fraction of energy contained with a given bandwidth window.

In some cases, the spectrum and peak brigthness will be optimized by using fewer undulators than required to reach full saturation. Including more undulators can result in high-current portions of the electron bunch radiating in the SASE regime and spoiling the quality of the seeded output signal.

In all of the examples shown, it is clear that suppressing the microbunching instability as much as possible is crucial to optimizing performance when using either self-seeding or external seeding, whereas for SASE the broad spectrum tends to cover up the impact of microbunching at moderate levels. For the EEHG scheme, it was found to be important to reduce wake field forces within the initial bunching section of the beamline by doubling the beam pipe diameter.

ACKNOWLEDGMENT

REFERENCES

[1] G. Marcus, Y. Ding, P. Emma, Z. Huang, T. Raubenheimer, L. Wang, and J. Wu. FEL simulation and performance studies for LCLS-II. In *Proc. 36th Int. Free Electron Laser Conf.*, pages 456–460, Basel, Switzerland, 2014. JACoW. TUP032.

[2] R. Bonifacio, L. De Salvo, P. Pierini, N. Piovella, and C. Pellegrini. Spectrum, temporal structure, and fluctuations in a high-gain free-electron laser starting from noise. *Phys. Rev. Lett.*, 73:70–73, 1994.

[3] J. Feldhaus, E.L. Saldin, J.R. Schneider, E.A. Schmeidmiller, and M.V. Yurkov. Possible application of x-ray optical elements for reducing the spectral bandwidth of an x-ray SASE FEL. *Optics Commun.*, 140:341–352, 1997.

[4] G. Geloni, V. Kocharyan, and E. Saldin. A novel self-seeding scheme for hard x-ray FELs. *Journal of Modern Optics*, 58:1391–1403, 2011.

[5] D. Ratner, R. Abela, J. Amman, C. Behrens, D. Bohler, G. Bouchard, C. Bostedt, M. Boyes, K. Chow, D. Cocco, et al. Experimental demonstration of a soft x-ray self-seeded free-electron laser. *Phys. Rev. Lett.*, 114:054801, 2015.

[6] E. Hemsing, M. Dunning, C. Hast, T.O. Raubenheimer, S. Weathersby, and D. Xiang. Highly coherent vacuum ultraviolet radiation at the 15th harmonic with echo-enabled harmonic generation technique. *Phys. Rev. ST Accel. Beams*, 17:070702, 2014.

[7] Z. Zhang, Y. Ding, W.M. Fawley, Z. Huang, J. Krzywinski, A.A. Lutman, G. Marcus, A. Marinelli, and D. Ratner. Microbunching-induced sidebands in a seeded free-electron laser. In *These Proceedings: Proc. 37th Int. Free Electron Laser Conf.*, Daejeon, Korea, 2015. JACoW. WEP084.

[8] J. Qiang, R.D. Ryne, M. Venturini, A.A. Zholents, and I.V. Pogorelov. High resolution simulation of beam dynamics in electron linacs for x-ray free electron lasers. *Phys. Rev. ST Accel. Beams*, 12:100702, 2009.

[9] G. Penn et al. FEL simulation and performance studies for LCLS-II. In *Proc. 36th Int. Free Electron Laser Conf.*, pages 223–226, Basel, Switzerland, 2014. JACoW. TUP032.

[10] K. Flöttmann. Astra: A space charge tracking algorithm. Technical report, DESY, Hamburg, 2000. User's manual available at http://www.desy.de/ mpyflo/.

[11] M. Borland. Elegant. Report LS-287, Advanced Photon Source, 2000.

[12] G. Marcus, Y. Ding, P.J. Emma, Z. Huang, H.-D. Nuhn, T. Raubenheimer, L. Wang, J. Qiang, and M. Venturini. High fidelity start-to-end numerical particle simulations and performance studies for LCLS-II. In *These Proceedings: Proc. 37th Int. Free Electron Laser Conf.*, Daejeon, Korea, 2015. JACoW. TUP007.

[13] S. Reiche. GENESIS 1.3: a fully 3D time-dependent FEL simulation code. *Nucl. Instr. Meth. A*, 429:243–248, 1999.

[14] LCLS-II Design Study Group. LCLS-II conceptual design report. Report LCLSII-1.1-DR-0001-R0, SLAC, January 2014.

[15] G. Stupakov. Using the beam-echo effect for generation of short-wavelength radiation. *Phys. Rev. Lett.*, 102:074801, 2009.